Non-linear patterns of eddy kinetic energy in the Japan/East Sea

O.O. Trusenkova, D.D. Kaplunenko,
S.Yu. Ladychenko, V.B. Lobanov
V.I.Il'ichev Pacific Oceanological Institute, FEB RAS
Vladivostok, Russia

PICES 2011 Meeting, POC/MONITOR/TCODE W4:
Recent advances in monitoring and understanding of Asian marginal seas:
5 years of CREAMS/PICES EAST-I Program

Motivation

Interacting modes of sea level variability in the Japan/East Sea

(Trusenkova et al., 2010)

Synchronous Mode | Gradient Mode | East – west Mode

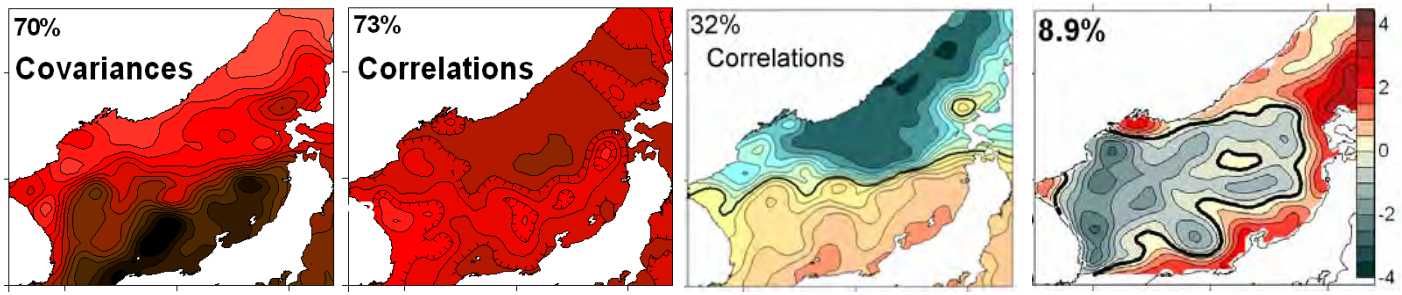

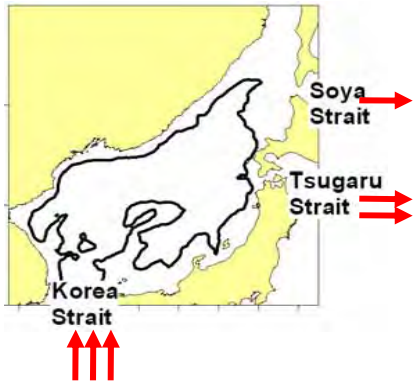

Interacting modes under the thermal forcing

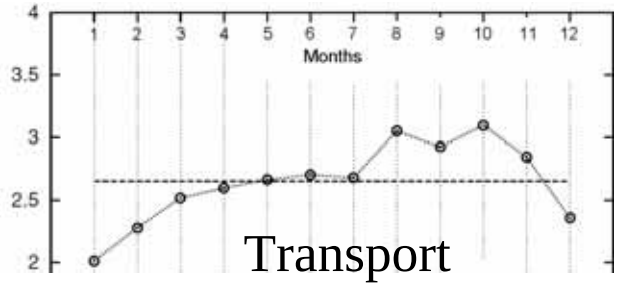

Transport in the Korea Strait (Fukudome et al., 2010)

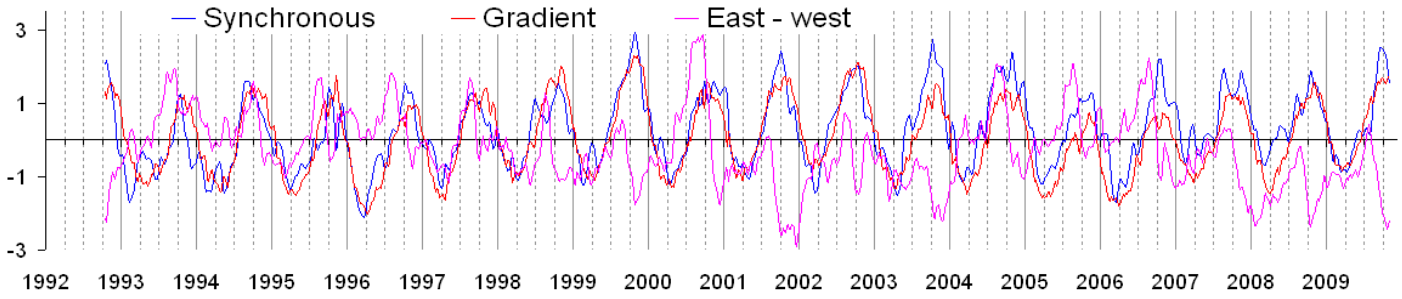

SLA and EKE

Synchronous Mode Gradient Mode

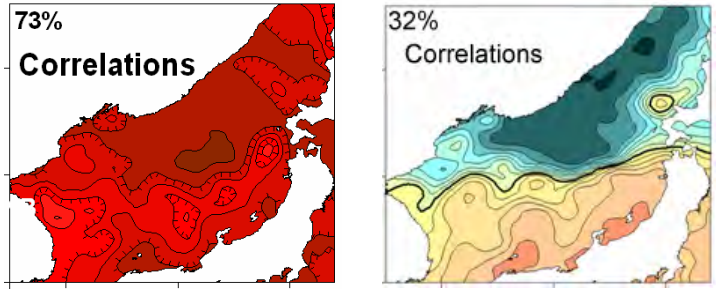

Seasonal highs and lows of the synchronous SLA and circulation strength under the thermal forcing in October and March.

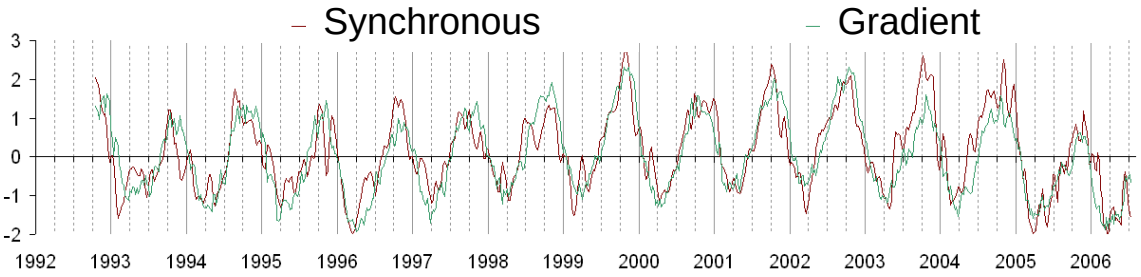

Previous EKE analyses: high (low) EKE in the southern (northern) sea (Cho et al., 2002), with the seasonal maximum in October and minimum in March (Son et al., 2010).

How to distinguish from the seasonal change of the circulation strength ?

Can EKE modes be non-orthogonal?

Purpose

To reveal probably interacting (non-orthogonal) modes of EKE variability by successive decompositions to EOF.

To compare EKE computed from the original altimetric SLA and from the residual SLA after the removal of the contributions from the seasonal SLA modes – synchronous oscillations and meridional gradient.

To analyze signatures of mesoscale structures in thermal contrasts on AVHRR infrared satellite imagery for interpretation of the EKE patterns.

Data

AVISO weekly reference 1/4°-gridded sea level anomalies, October 1992 - October 2009, 35.5°-48°N, 127.5°-142°E.

EKE = $(u'^2 + v'^2)/2$ where
$u' = -(g/f)\partial\eta/\partial y$, $v' = (g/f)\partial\eta/\partial x$, η - altimetric SLA → geostrophic & ergodic & spatial scales > 25 km.
(Noise level increased by differentiation.)

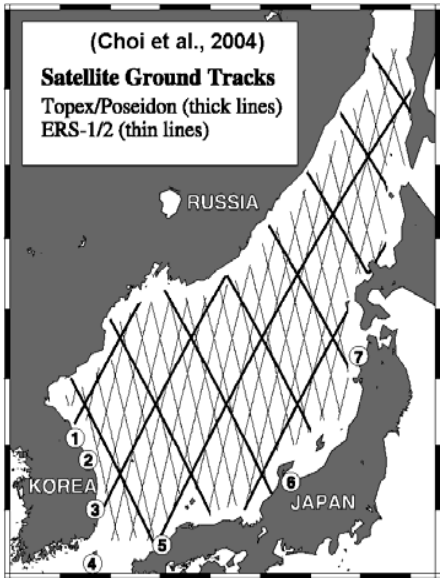

Filtering for noise removing, using Morler mother wavelet of the 6-th order, with the 20-week cut-off period → low-frequency EKE, with time scales > 2-4 months ~ persistent or frequent features.
Similar results for the cut-off periods of 9 and 13 weeks but lower eigenvalues.

Infrared satellite imagery NOAA AVHRR for July – October 2000 - 2008.

Removing the contribution of the seasonal sea level modes

Synchronous Mode | Gradient Mode | East – west Mode

SLA = 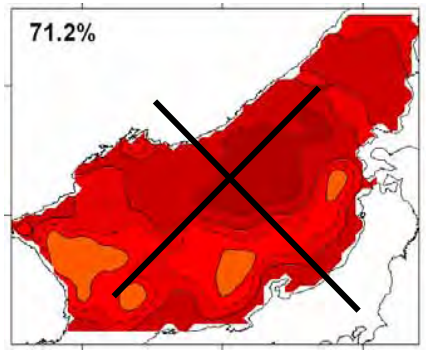

+ 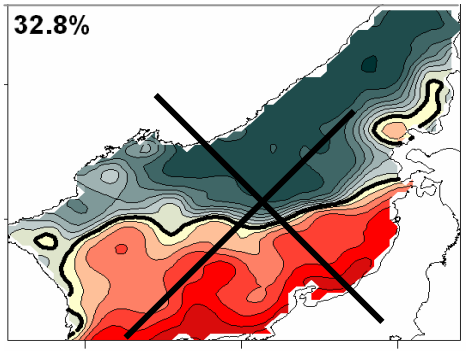

+ 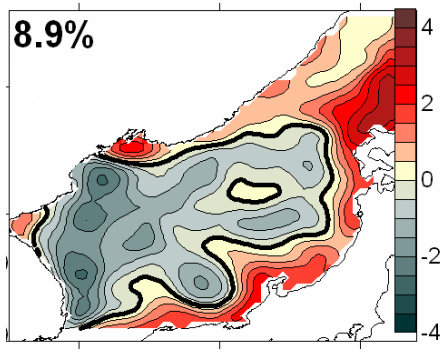

+ ε

Residual SLA

Residual SLA derived by subtraction of the contributions from the seasonal sea level modes

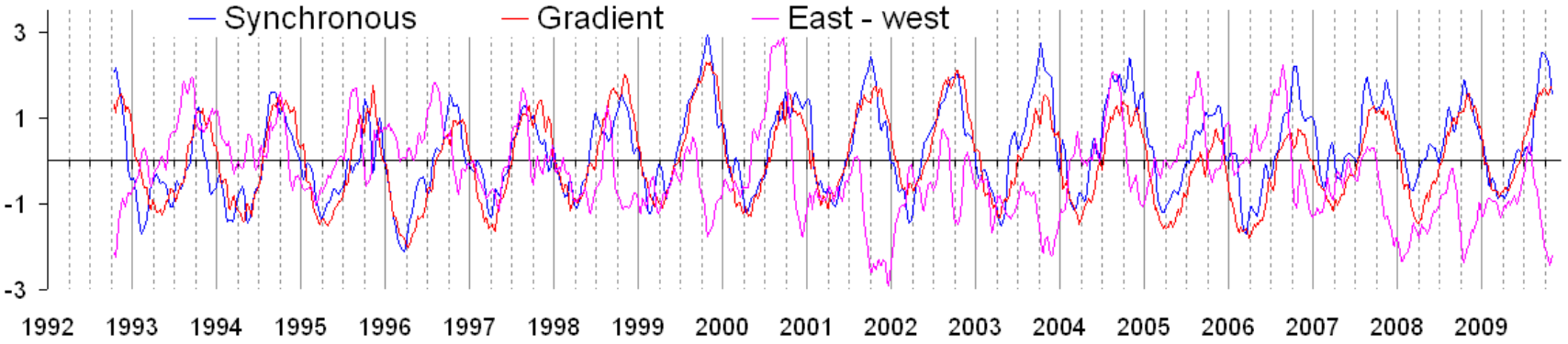

Mean EKE: maximum energy on mesoscale

EKE: from original SLA (O) from residual SLA (R)

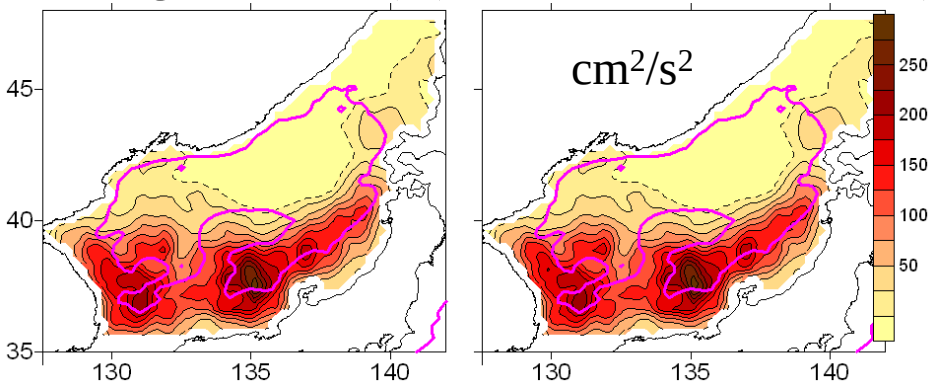

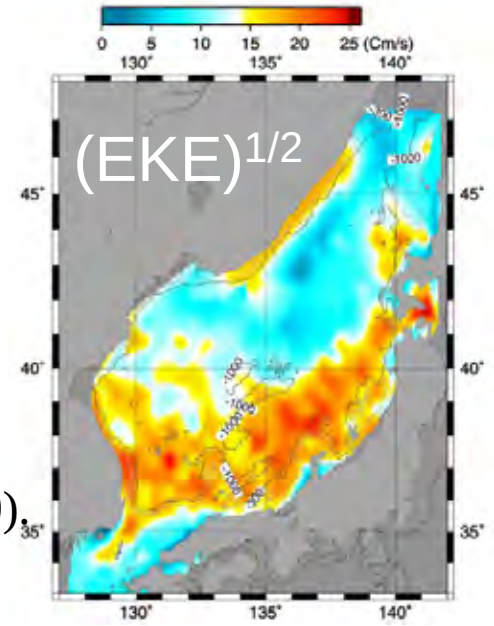

Correlated by > 0.95.

Spatial/temporal distribution in agreement with (Son et al., 2010).

Seasonal extremes in October and March.

Correlated with the seasonal sea level modes by ~ 0.8.

Altimetric EKE is 2-5 times lower than Argos EKE → contribution from barotropic eddies is important.

From Argos floats (15 m depth) (Lee and Niiler, 2005)

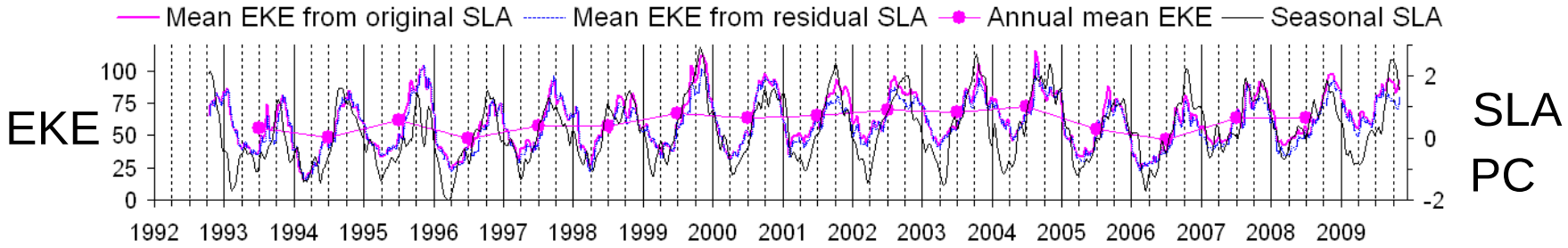

Techniques of EOF analysis

$X(r, t) = \sum A_k(r) \cdot B_k(t)$, where $X(r, t)$ – original signal, $A_k(r)$ is eigenvector from spatial correlation matrix, $B_k(t)$ is temporal coefficient (principal component).

Correlations, not covariances →

detection of small amplitude anomalies in the northern sea;

correlations ~ pre-normalization ~ pattern adjustment in the next decomposition.

Residual anomalies: $X_a(r, t) = X(r, t) - A_1(r) \cdot B_1(t)$.

Decomposition 1 (original SLA)

Removal of the EOF1 contribution

Decomposition 2 (residual SLA)

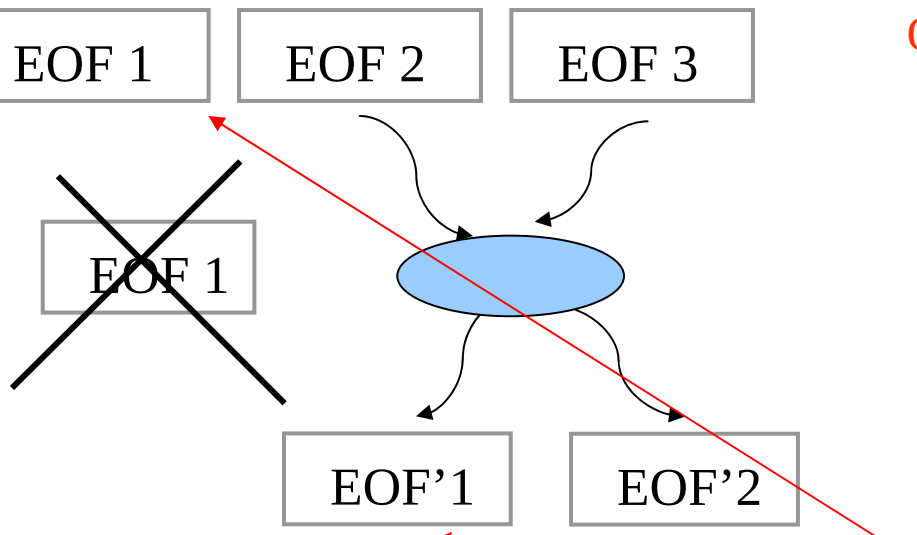

Orthogonal

Not necessarily orthogonal

This approach was applied to SST (Trusenkova et al., 2009) and SLA (Trusenkova et al., 2010).

Statistically significant modes from successive EOF decompositions

(EKE from residual SLA)

EKE	Mode	Eigenvalue (%)
R^1	#1 (R^1_1)	15.5±1.5
R^2 : Mode R^1_1 removed	#1 (R^2_1)	34.3±3.4
R^3 : Mode R^2_1 removed	#1 (R^3_1)	19.8±2.1
	#2 (R^3_2)	6.0±0.6
R^4: Mode R^3_1 removed	#1 (R^4_1)	18.8±1.8
	#2 (R^4_2)	6.0±0.6

Modes R^1_1 – R^4_1 account for more than 60% of the total variance

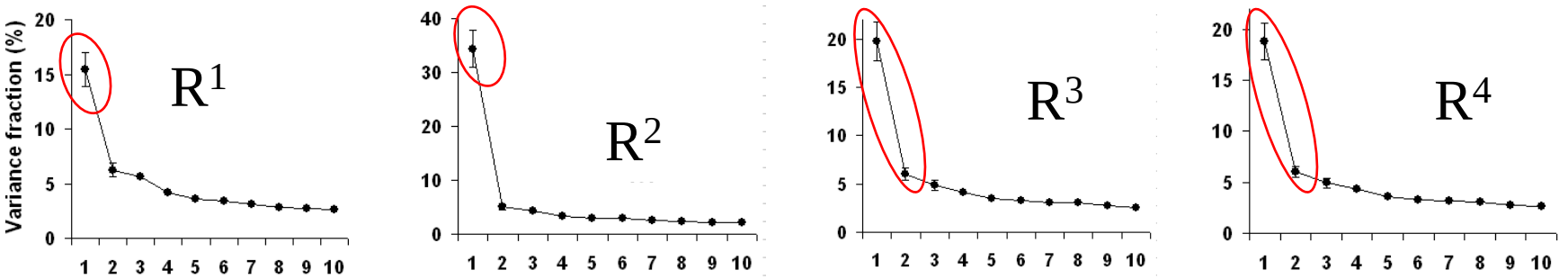

Leading EKE mode from the original and residual SLA

From original SLA

From residual SLA

(Seasonal change of the mean current strength is removed)

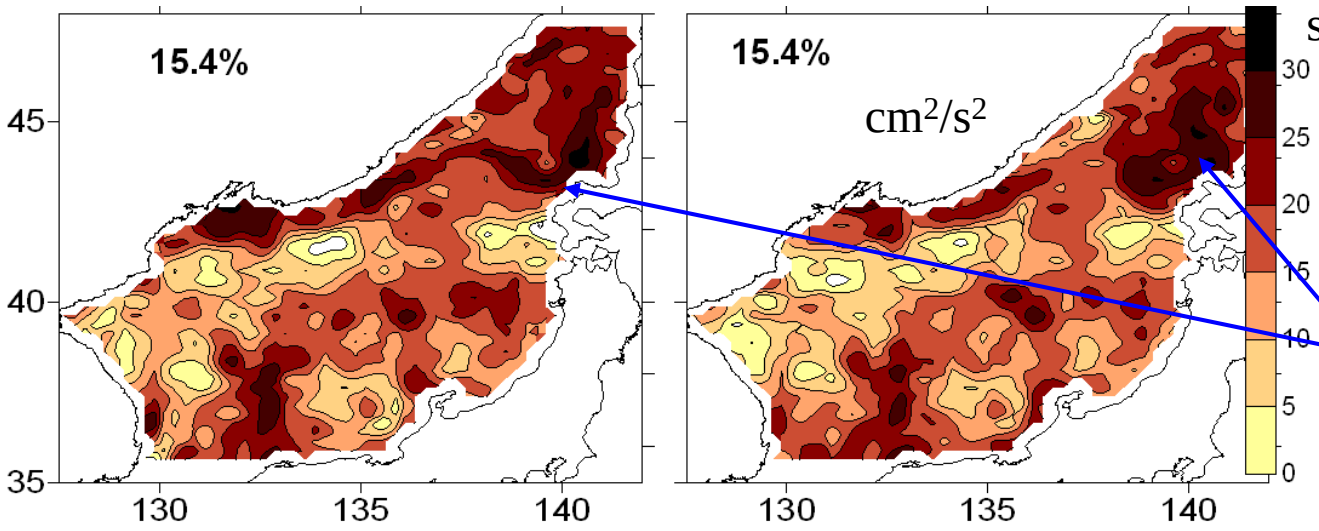

The same mode

Minor differences in spatial patterns

PC cross-correlation ~ 0.98, with mean EKE >0.96, with seasonal SLA ~ 0.8.

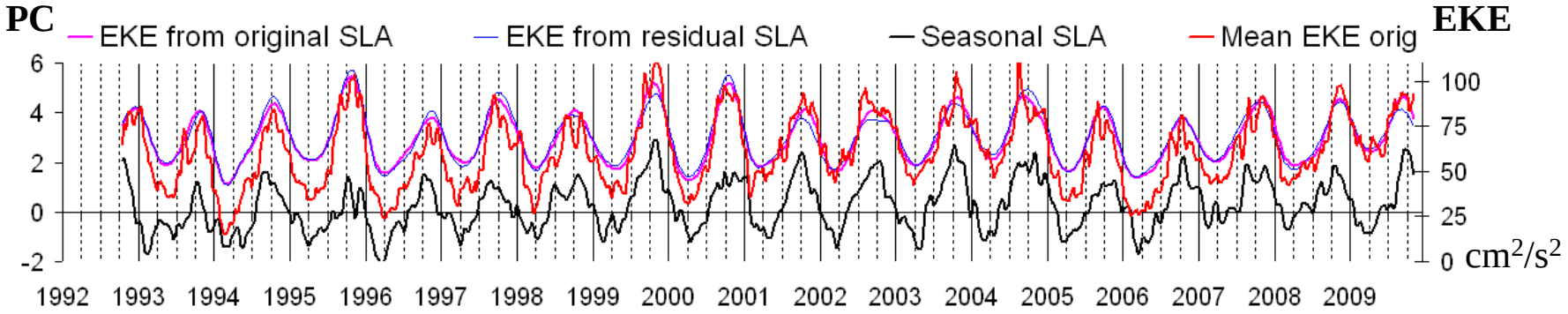

No trends over the whole record

Mean EKE: 0.9 cm^2/s^2 per year for 1993-2007 (Son et al., 2011),
~0.8 cm^2/s^2 per year for 1993-2009.

Low frequency mean EKE: <0.2 cm^2/s^2 per year

PC: no trend

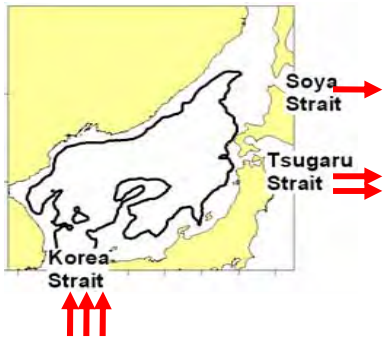

Mean EKE

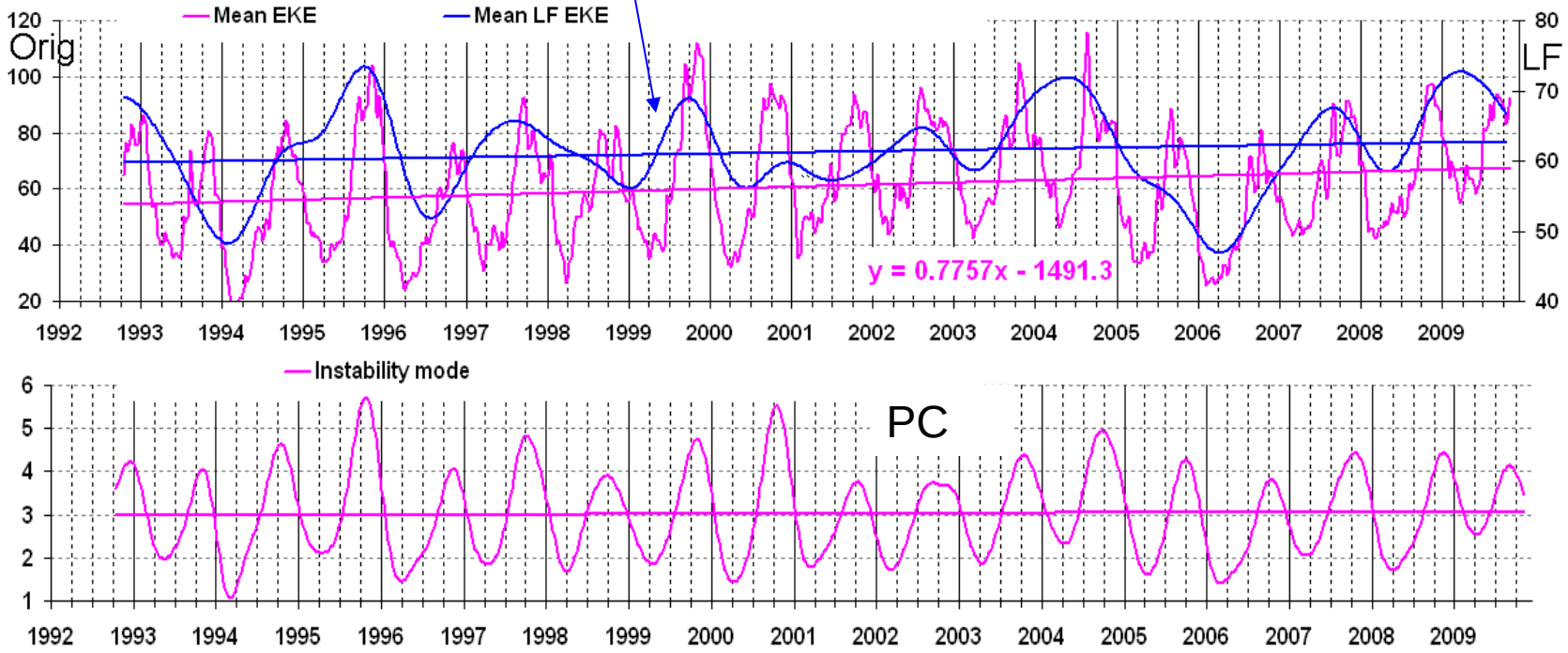

Excluding alongshore zones

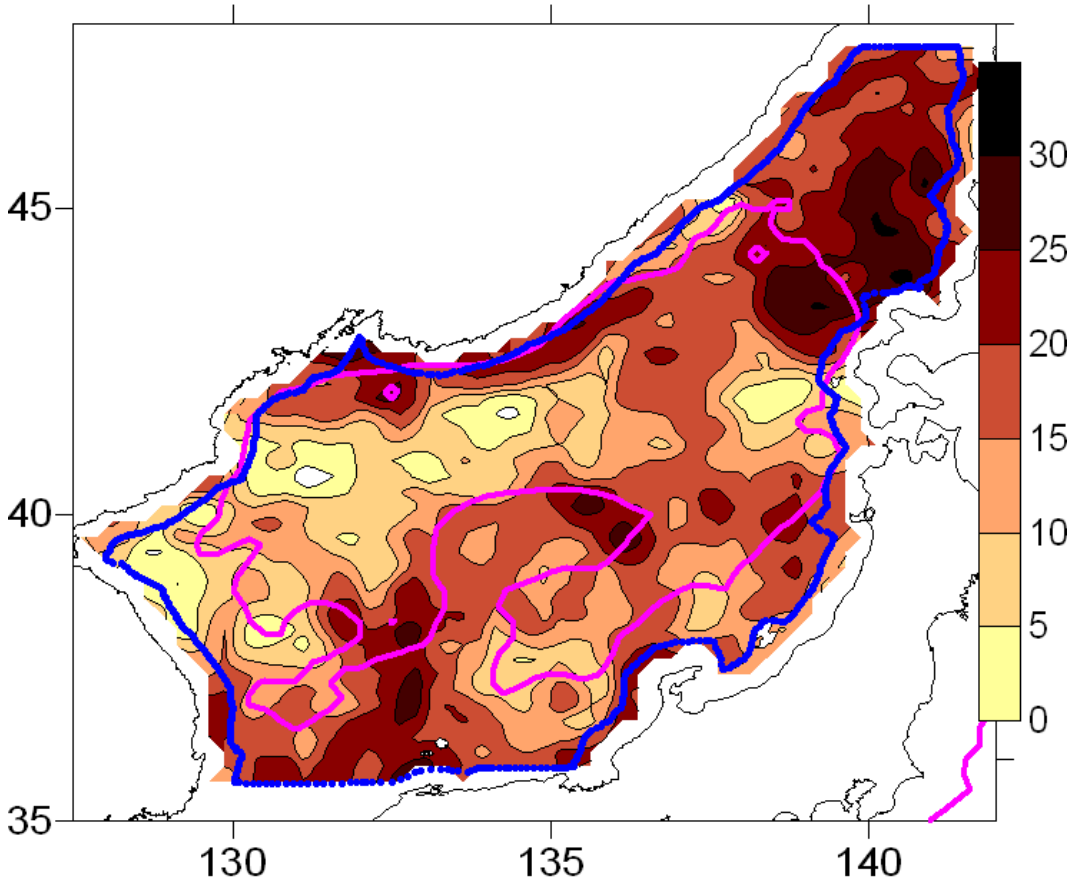

Δx, Δy ~ 25 km, SLA (η) ~ 50 km offshore, velocity and EKE ~ 60 km offshore.

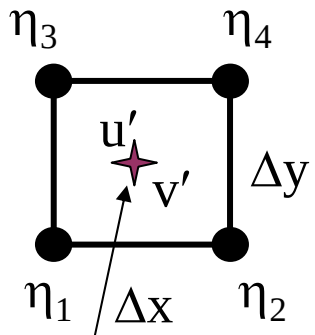

$u' = -(g/f)\Delta\eta/\Delta y$

$v' = (g/f)\Delta\eta/\Delta x$

$E_m = (u'^2 + v'^2)/2$

Checked mesh: SLA (η) in the corners, velocity and EKE in the center.

Instability of mean currents

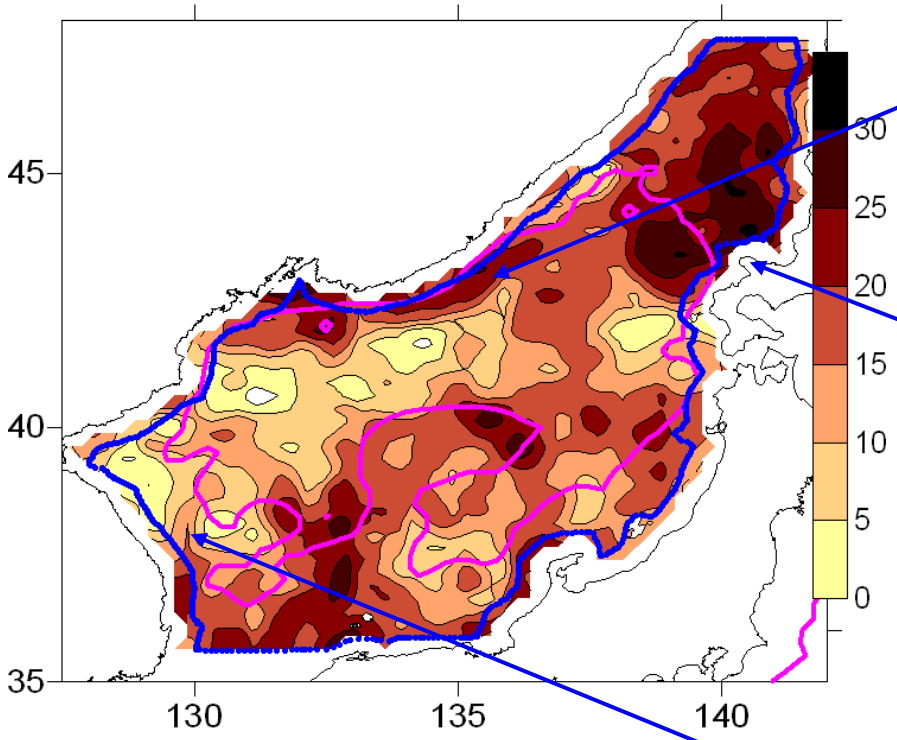

Primorye Current

TWC branching off Hokkaido

EKWC and EKWC Extension

From surface drifters

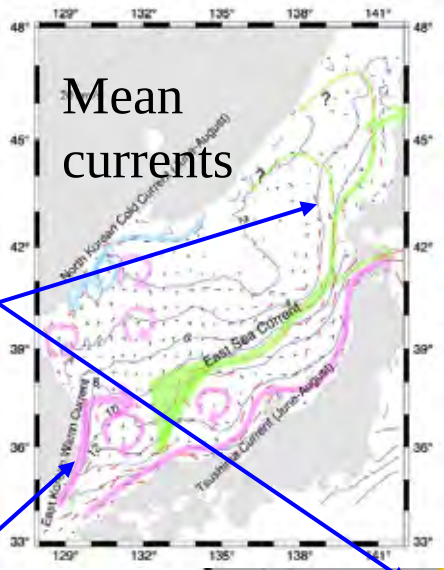

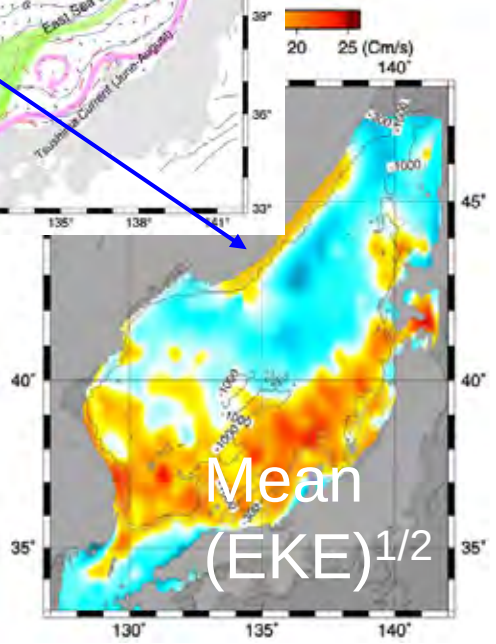

(Lee and Niiler, 2005)

Interactions with bathymetry

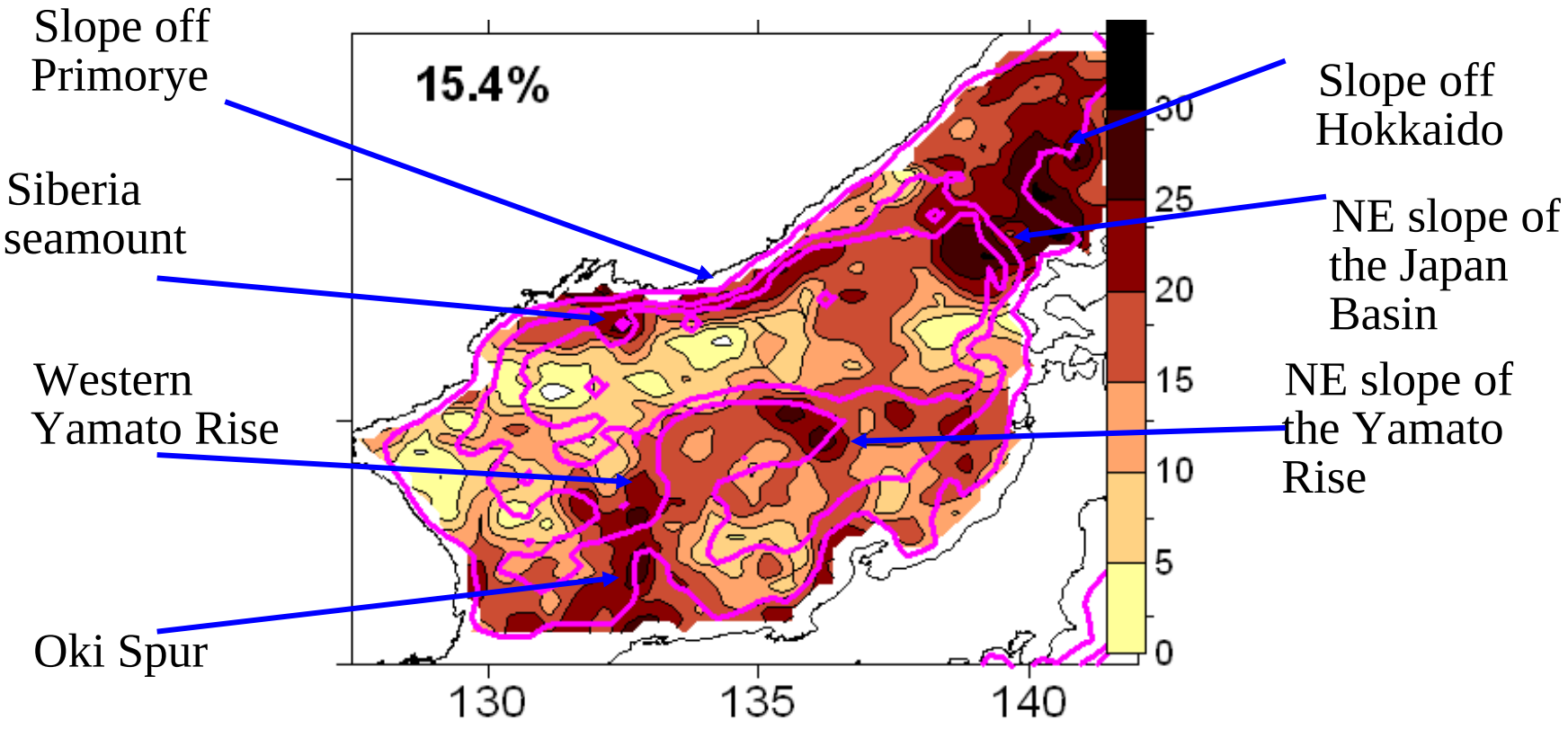

The 500, 2000, and 3000 m isobaths

Unobserved structures

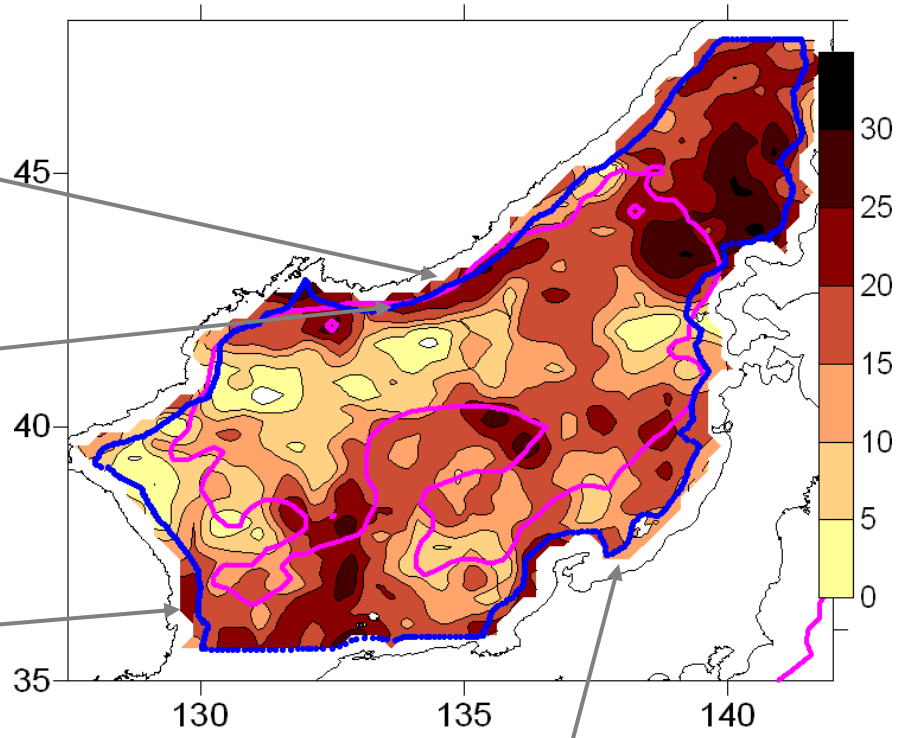

Slope eddies

Partly the Primorye Current

EKWC

Nearshore branch of the Tsushima Warm Current

Zonal and meridional EKE

$$EKE = (u'^2 + v'^2)/2$$

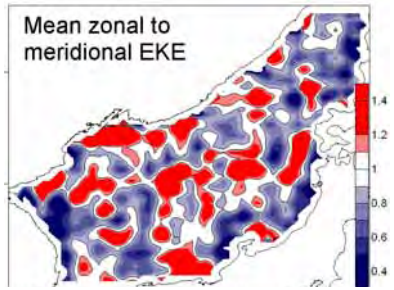

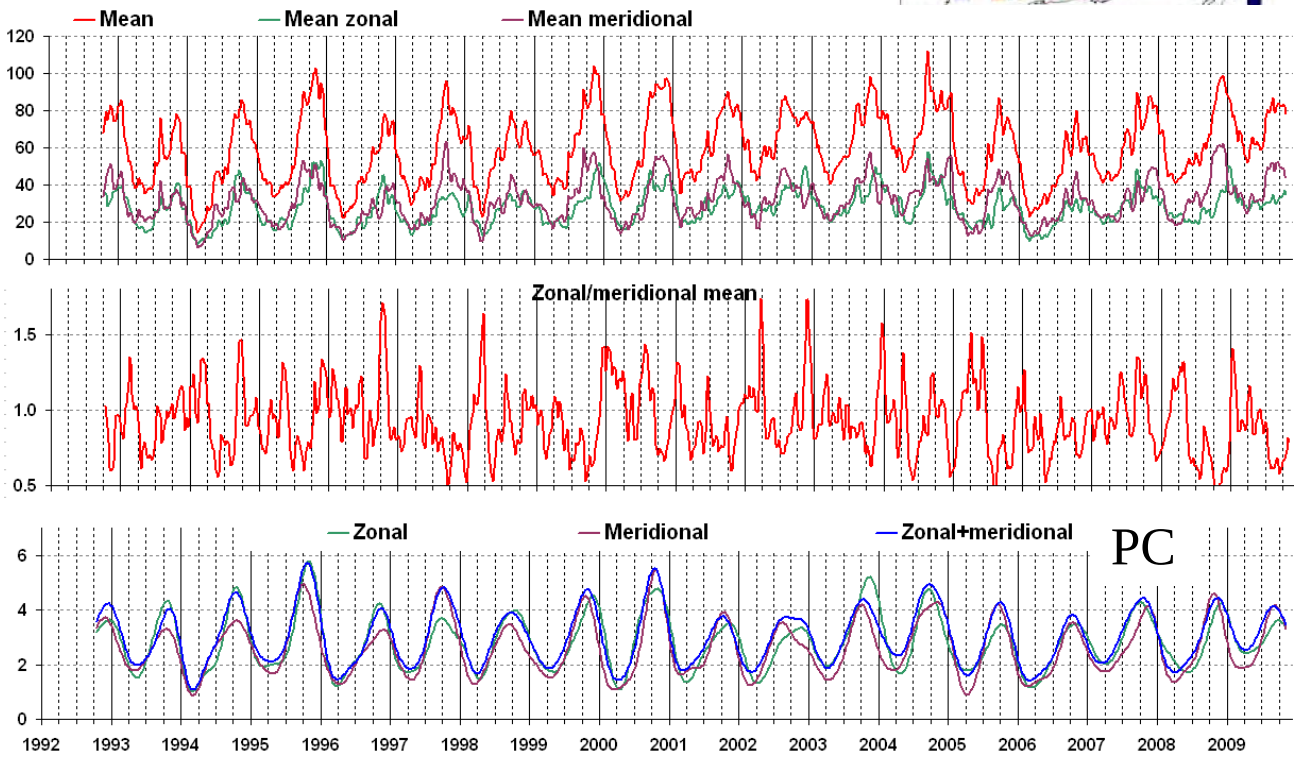

The same seasonal signal

Mode 1

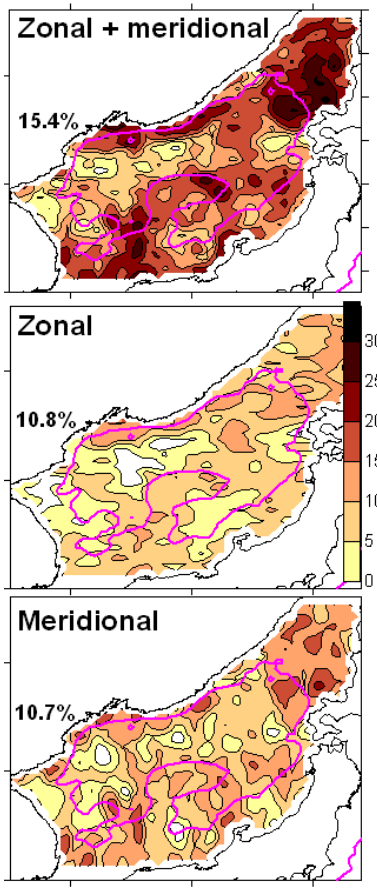

Spatial maxima linked to dynamic and topographic structures

Baroclinic instability

In the Gulf Stream region EKE peaks in summer (August), although the ocean is most baroclinically unstable (T_{bc} is largest) in winter, but dissipation is also reduced in summer (Zhai et al., 2008).

EKE is largest in winter in most of the subarctic gyres due to barotropic instability.

Baroclinic eddy growth time scale (Stammer, 1998)

$$T_{bc} = \sqrt{Ri} / f$$

$$\overline{\mathrm{Ri}} = \overline{N^2} / \overline{|\partial u/\partial z|^2}$$

$$N = \sqrt{-\rho_0^{-1} g \partial\rho/\partial z}$$

$$|\partial u/\partial z| = \frac{g}{\rho_0 f}\sqrt{(\partial\rho/\partial x)^2 + (\partial\rho/\partial x)^2}$$

Mean T_{bc} in the 300 м layer (Son et al., 2011)

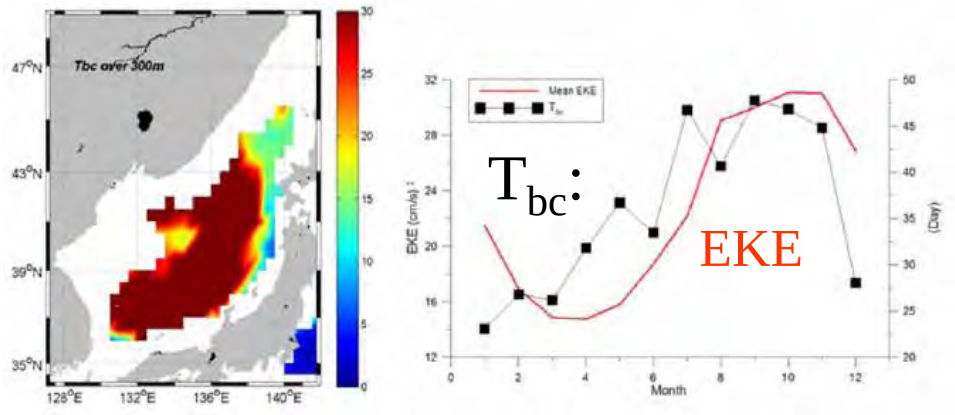

Seasonal variation similar to that in the oceanic subtropical gyres

Barotropic instability in the Japan/East Sea

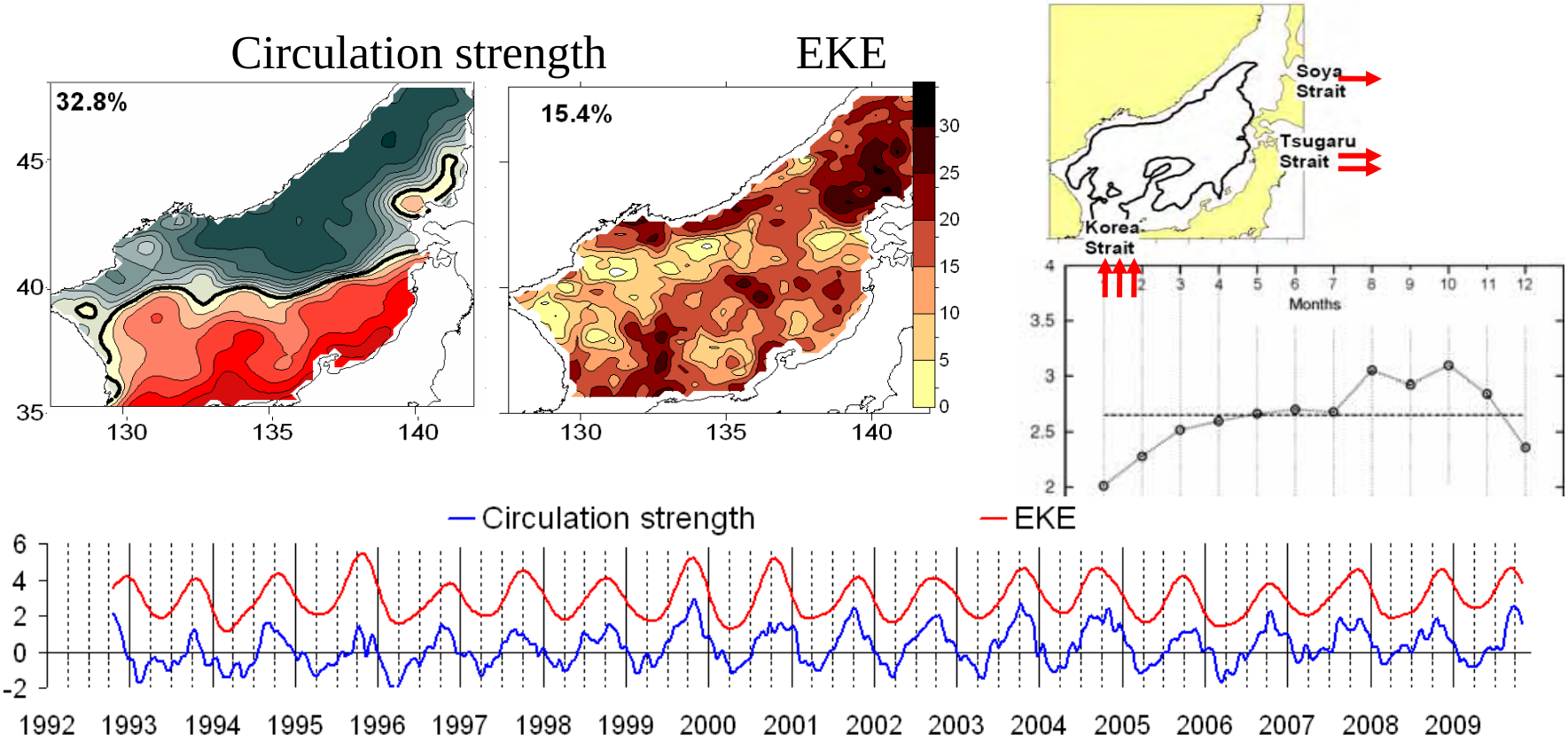

Seasonal variation of the circulation strength and EKE are the same → increase of barotropic instability due to the current shear.

Synchronized barotropic and baroclinic instability as a possible cause of the very intense mesoscale dynamics in the Japan Sea

Adjustment mode: convergence to the mean EKE

From original SLA From residual SLA

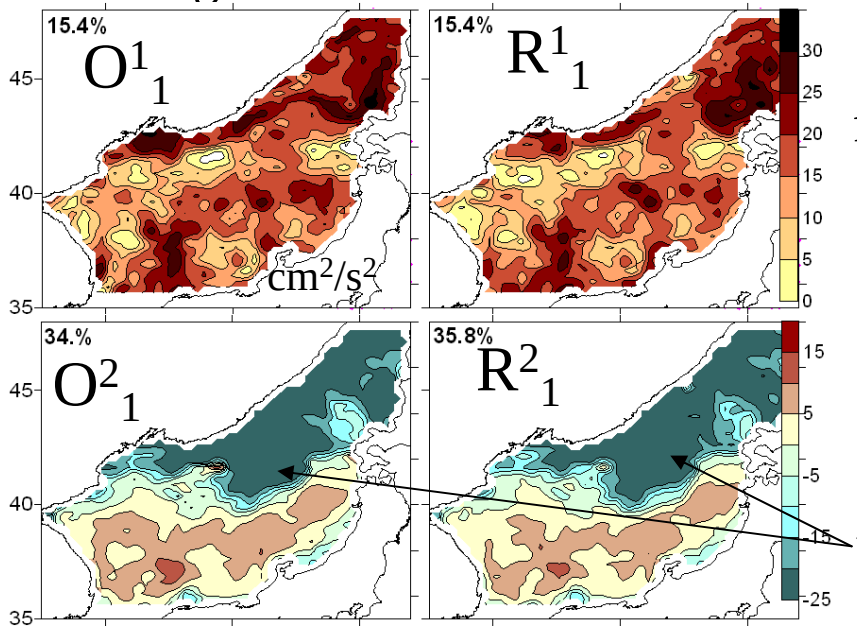

Mean EKE

from original SLA from residual SLA

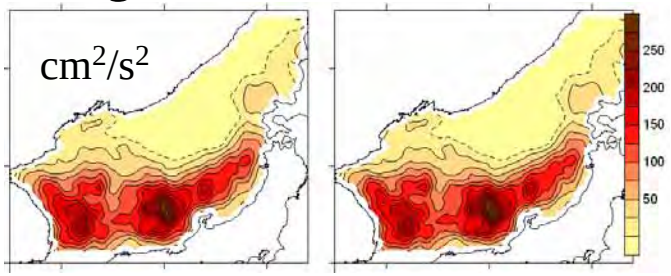

< 5% variance in the northern core

$R^1 1$: uniform northern core ~ $O^1 1$ spatial structure remains.

These modes are from different decompositions!

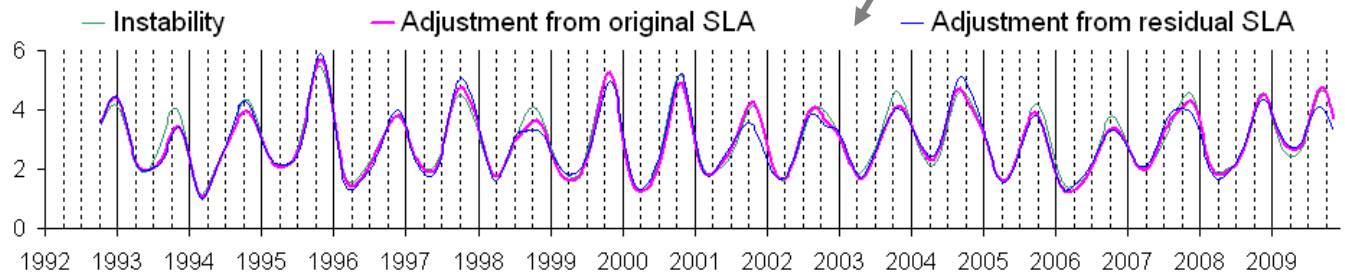

Correlation

R^1_1/R^1_2 ~ 0.98

Primorye Mode

Spatial maximum off the Primorye coast

Adjustment for convergence to mean EKE

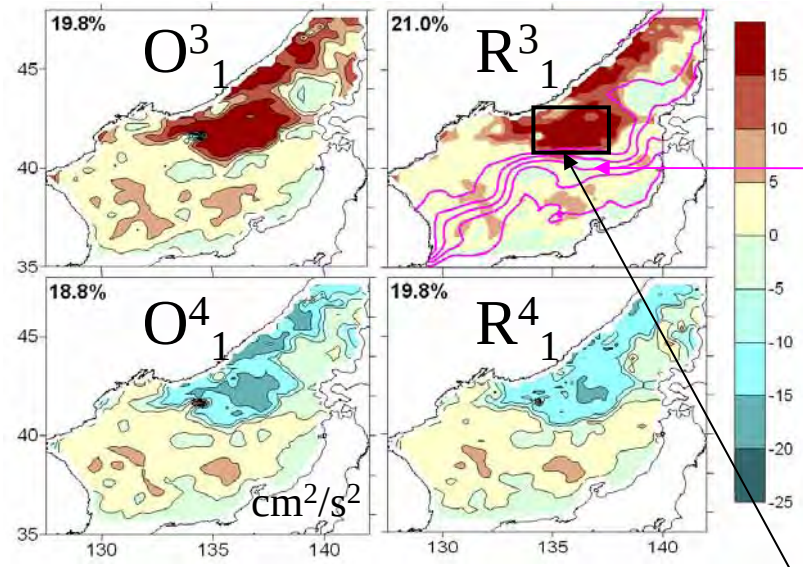

Subarctic front in simulated SSH

From original SLA From residual SLA

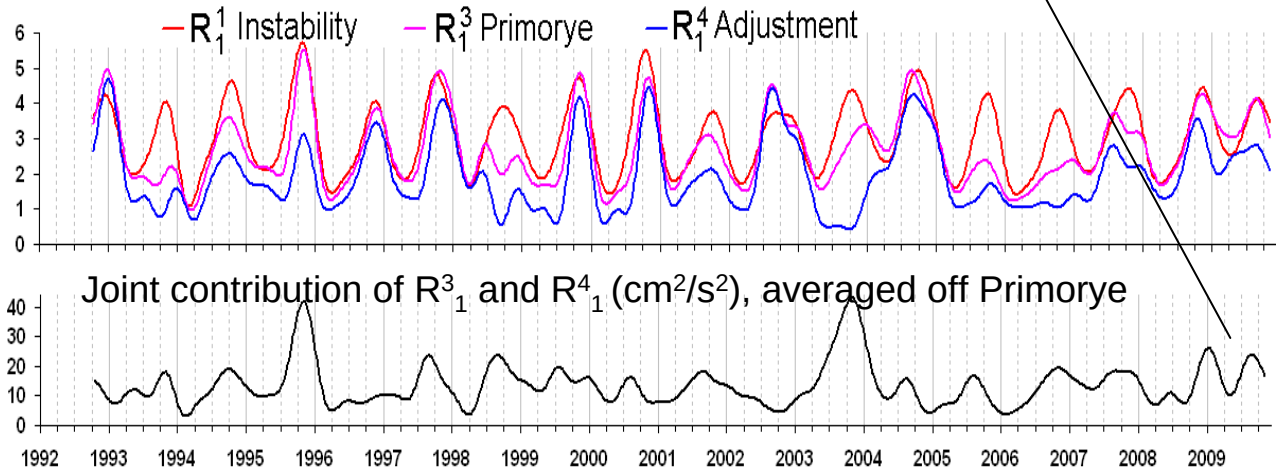

Primorye Mode: temporal variation

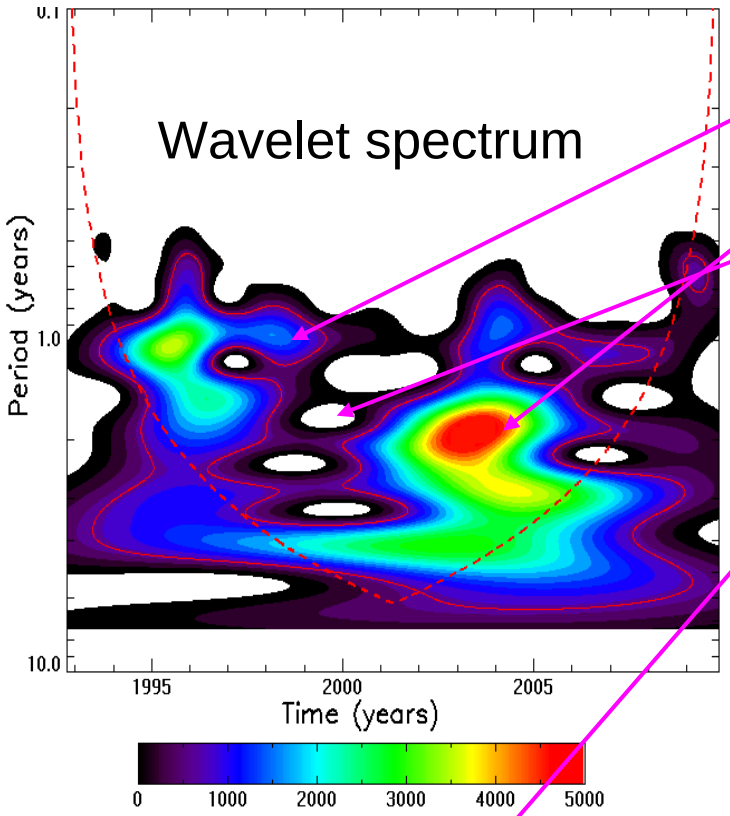

Strong seasonal signal before 1997

QB variability after 2000

Low EKE in 1998-2000

Extreme EKE in 1995 and 2003

Irregular temporal variation → wind forcing?

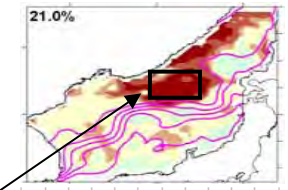

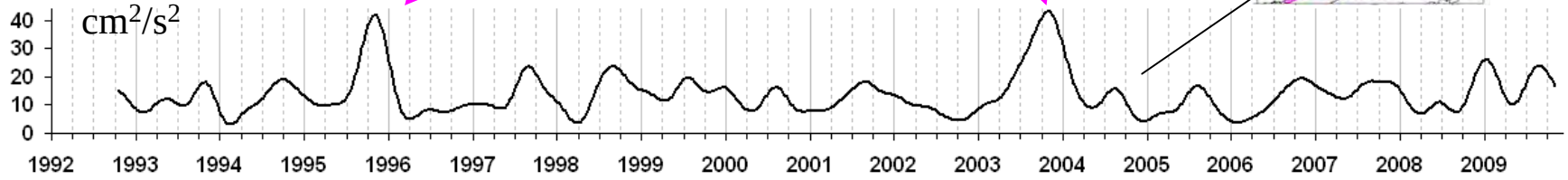

Synoptic structures off the Primorye coast
(from infrared satellite images in July through October)

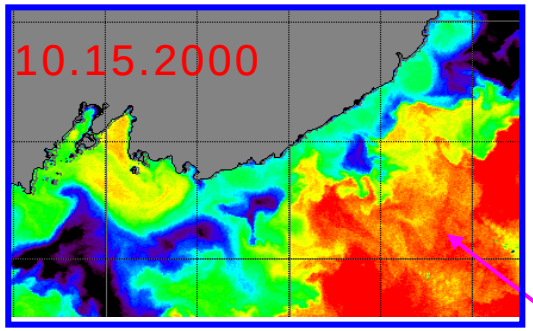

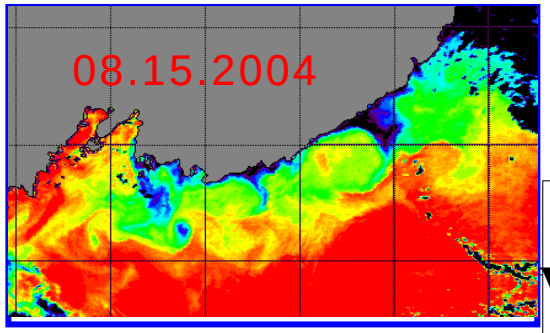

Slope eddies
(30-60 km)

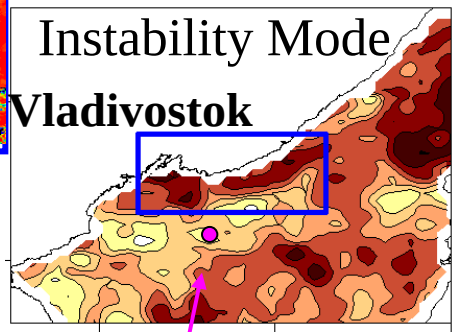

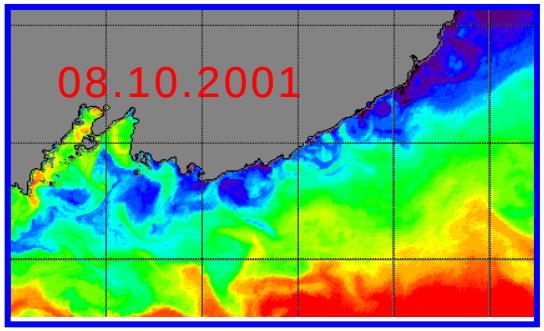

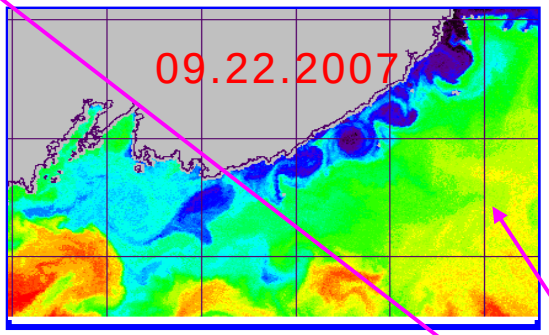

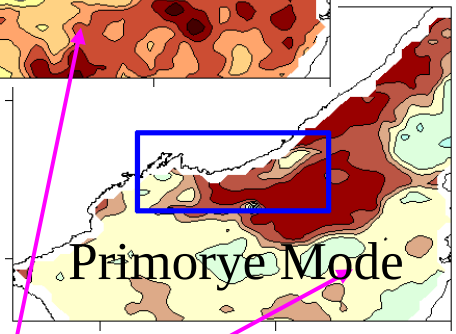

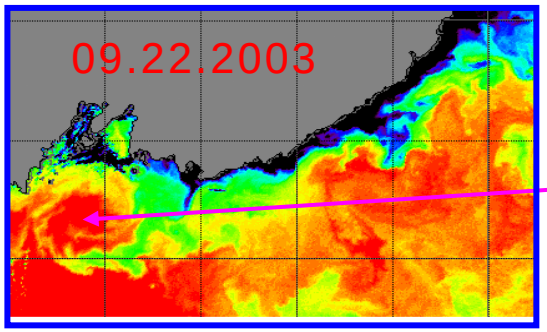

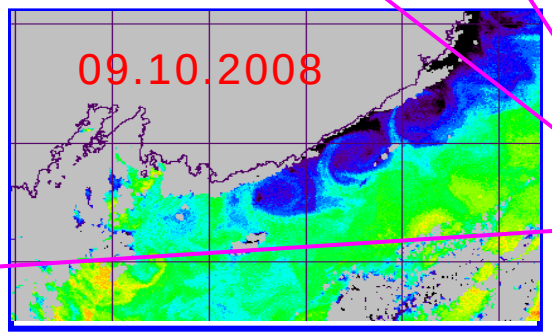

Variety of structures

Cold water in blue,
warm water in red.

Eddy life time from days through 1.5 months
→ EKE pattern reflects repeated structures.

Peter the Great Bay and adjacent area

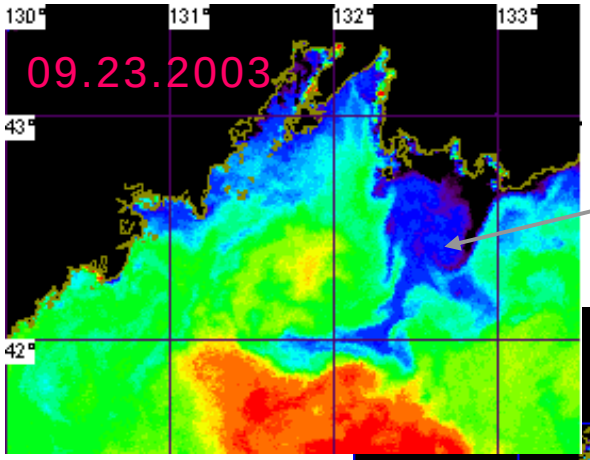

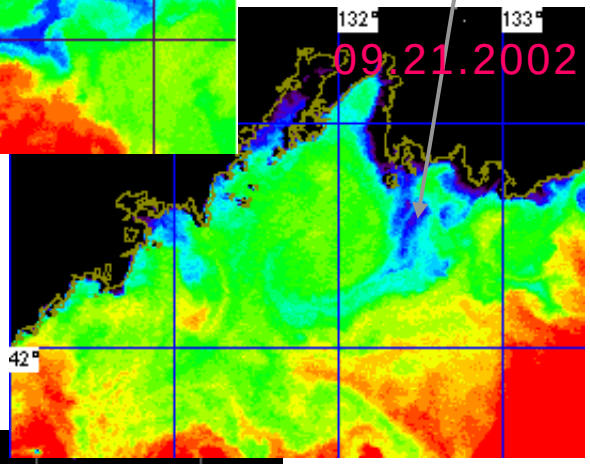

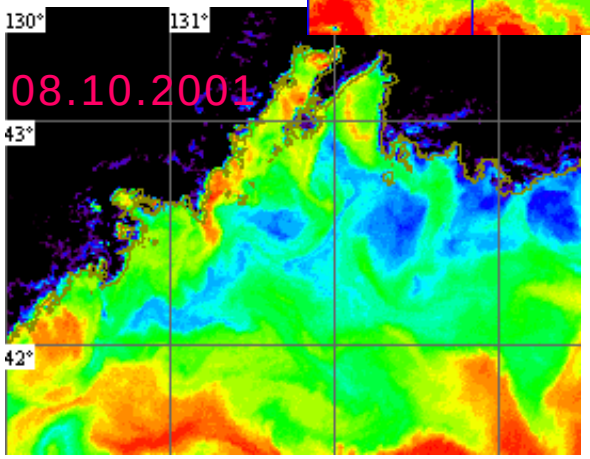

Interaction of upwelling with an eddy

Local maximum over the Siberia Seamount

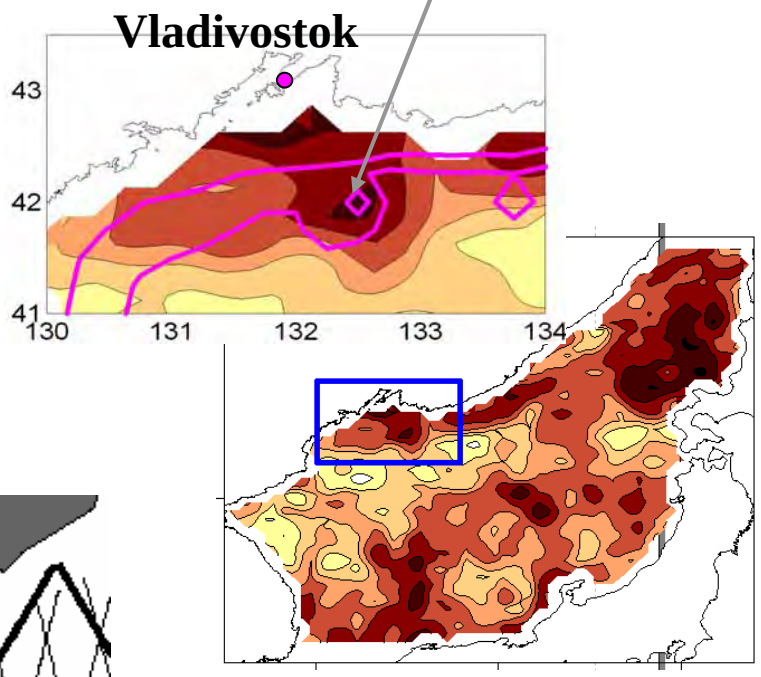

T/P & Jason tracks are bold,
ERS & EnviSAT are thin.

Mesoscale eddies in early fall in the northern sea

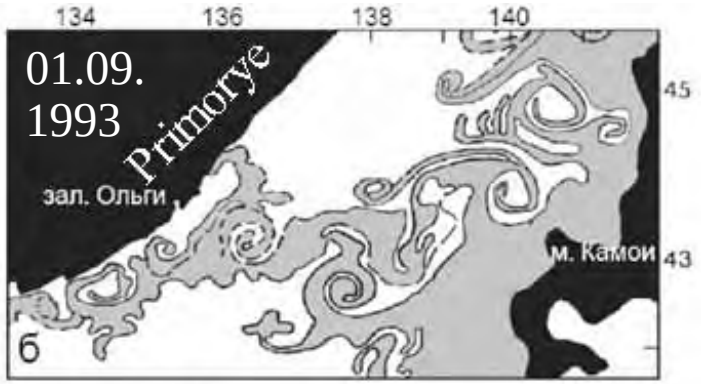

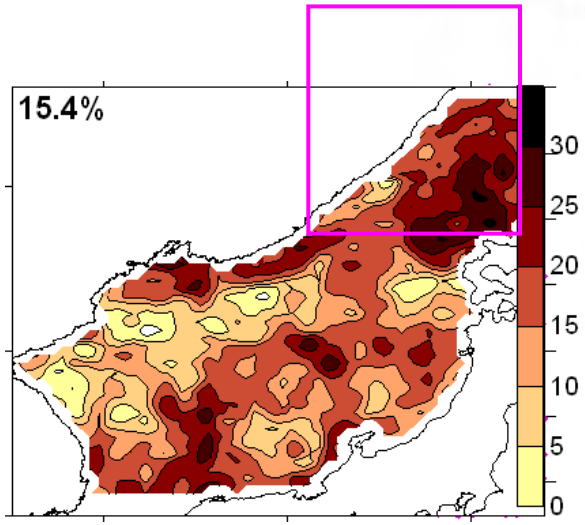

Tatarsky Strait

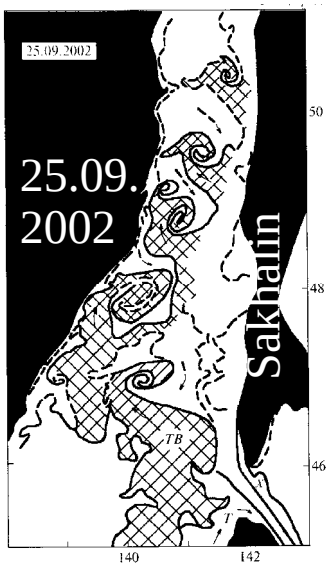

(Nikitin and Yurasov, 2008)

Wind strengthening and AC curl in fall (from QSCAT)

Monthly wind stress & stress curl

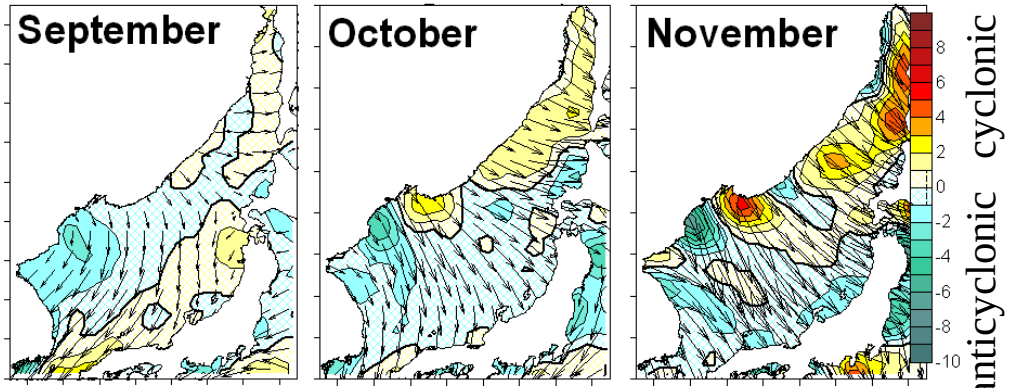

$\times 10^{-8}$ dyn/cm^3

EOF analysis

Low-pass filtered curl, 40-day cut-off.

AC curl in late winter/spring and fall; cyclonic to zero oscillating curl in late summer (Trusenkova, 2010).

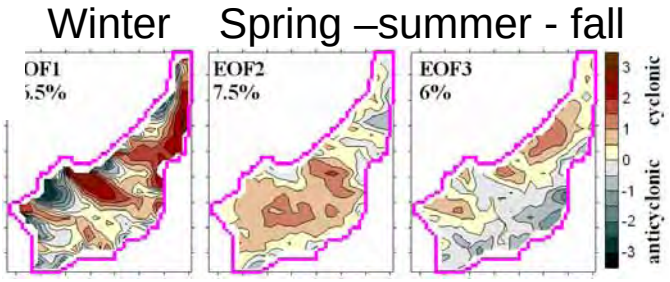

Wind strengthening and AC curl in fall (south of 43° → steering of mesoscale dynamics?

PC ($\times 10^{-8}$ dyn/cm^3)

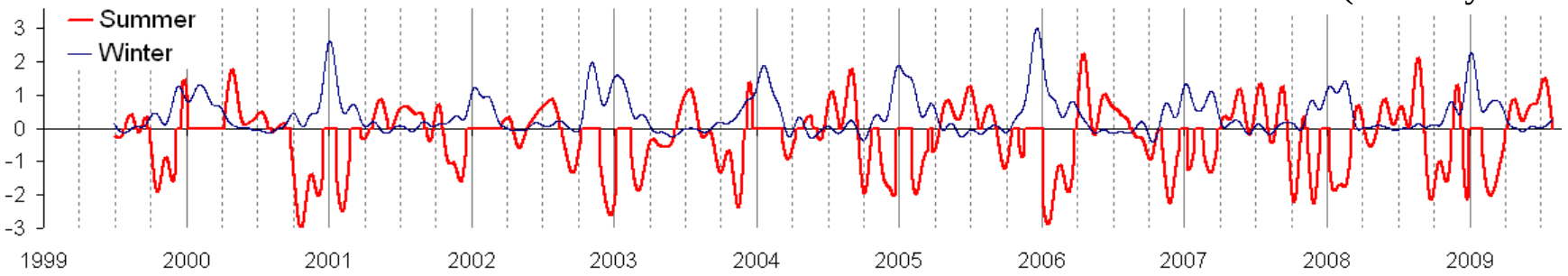

Blue curve is for the contribution from the winter mode and red curve from two summer modes.

East - west seesaw in EKE and SLA

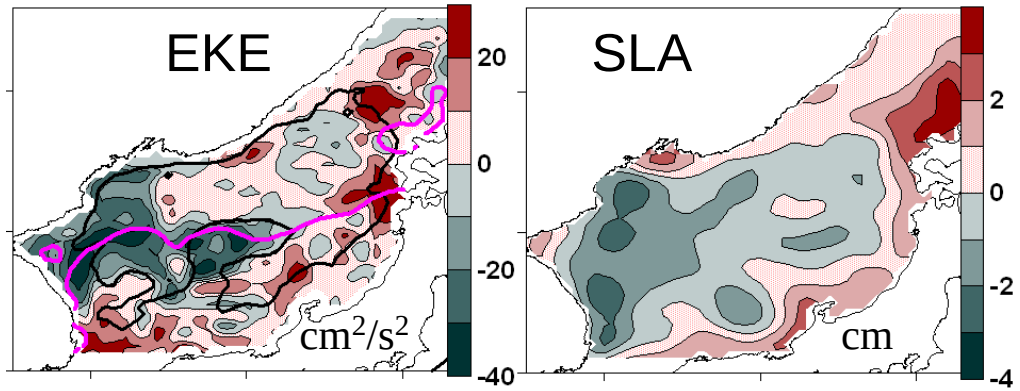

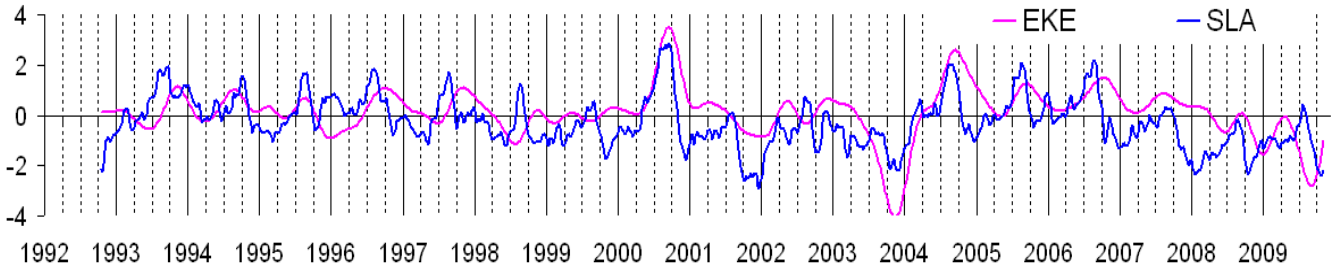

EKE and SLA – spatial patterns similar but not quite the same.
SLA seasonal extremes in late summer and in fall through spring;
EKE interannual variability only.
Similarity with SLA since 2001, with correlation ~ 0.71.

Extreme events in 2000 (strong positive phase) and
in 2003 (strong negative phase). Extreme Primorye Mode in 2003.

Pathways of the northward transport of warm water from the Korea Strait

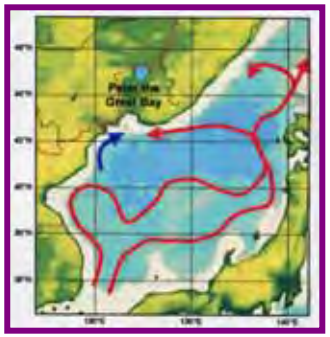

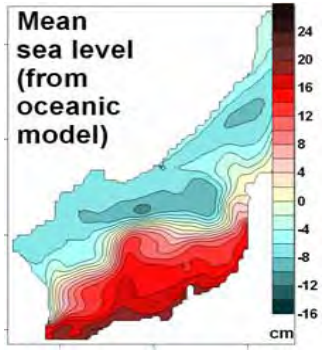

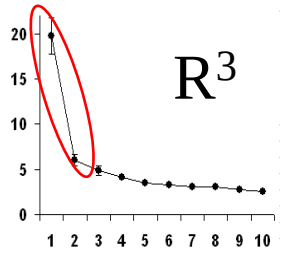

Systems of warm eddies in the northwestern Japan Sea (from infrared satellite imagery)

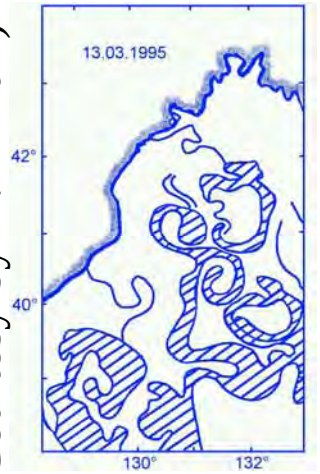

(Courtesy by A. Nikitin)

Subarctic boundary

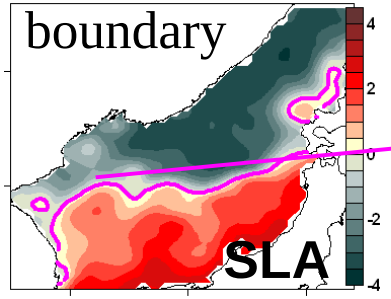

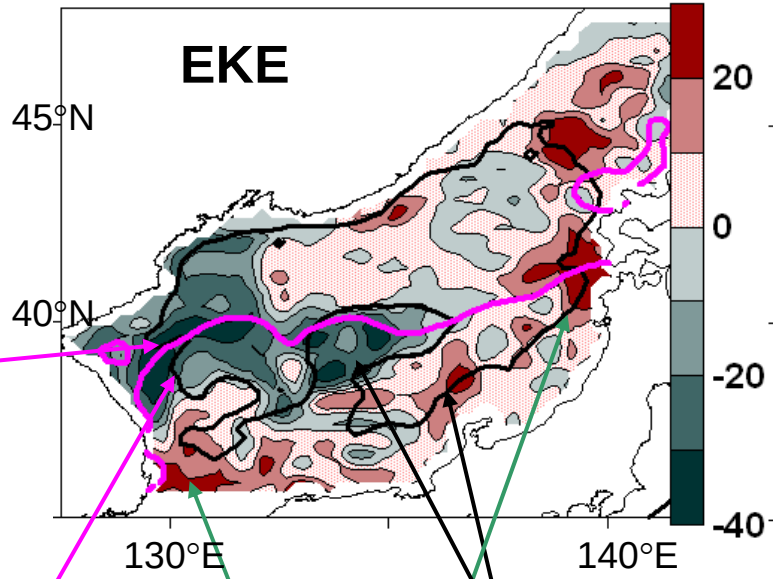

Flow patterns in the southwestern Japan Sea: strong EKWC (Inertial Boundary Current – IBC – pattern); eastward flow (TWC pattern), strong or weak Ulleung Warm Eddy (UWE patterns). SLA by color, drifter tracks by contours (Lee and Niiler, 2010).

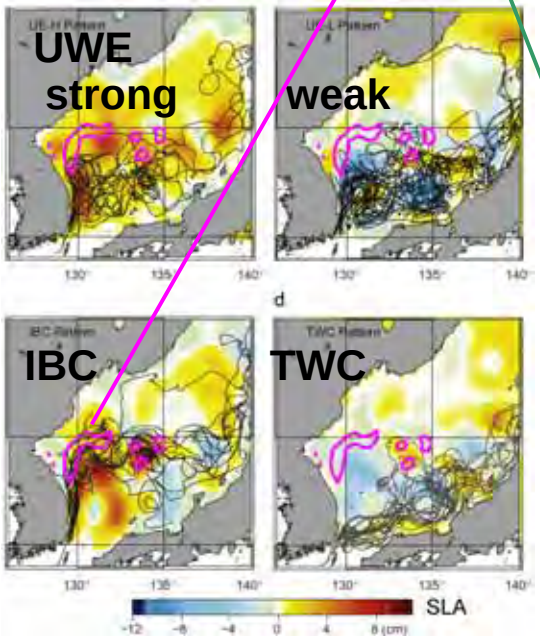

Opposite anomalies in the Yamato Rise and Yamato Basin

Korea and Tsugaru Straits: in-phase EKE → concurrent transport anomalies?

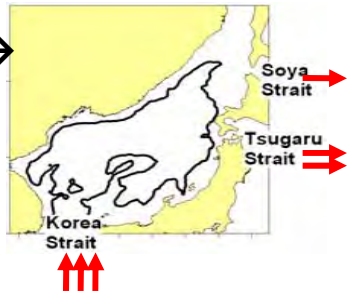

QB and interannual variability

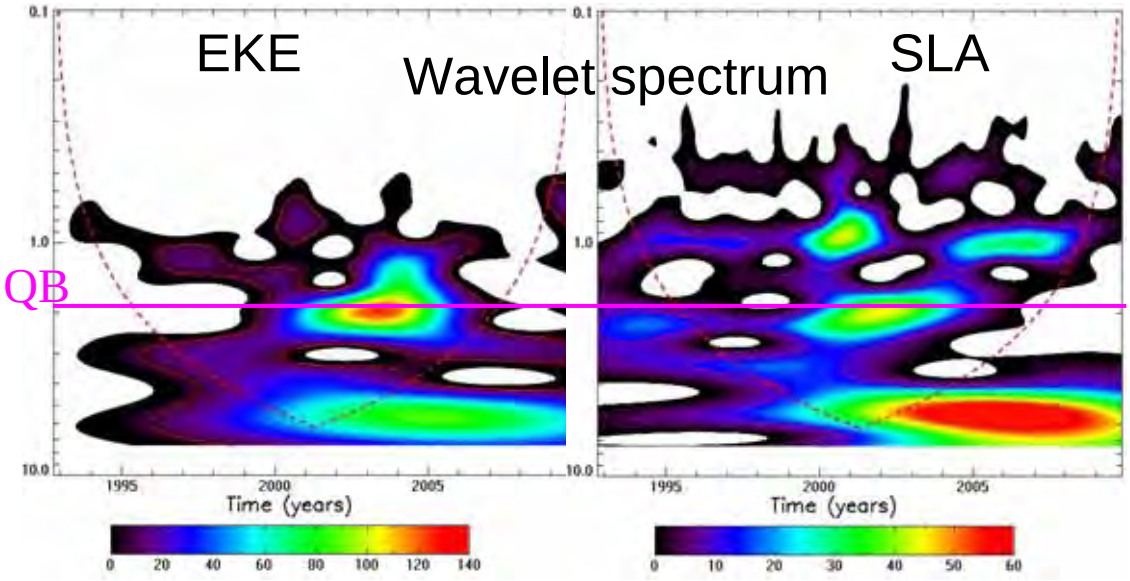

Different regimes (after 2000):
Positive phase in 2000, 2004-2006: increased EKE in the eastern JES.

Negative phase in 2001-2003 and 2007-2009:
increased EKE the western JES.

Decreasing trend since 2007 – manifestation of another regime?.

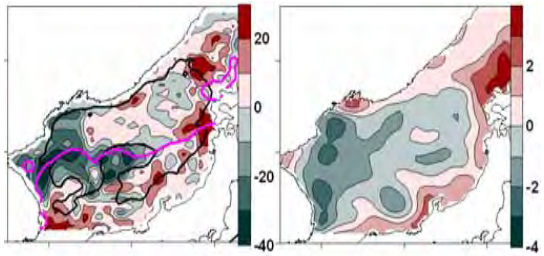

QB variability in the southern JES (path variations of the TWC; Hirose and Ostrovskii, 2000; Choi et al., 2004).

Possible forcing: atmospheric QB variability.

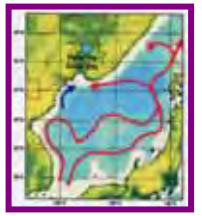

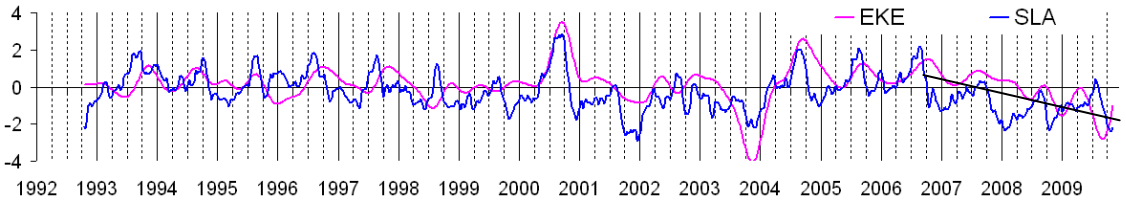

No trend over the whole period

Conclusion

- Interacting EKE modes in the Japan/East Sea.
- The same seasonal signal in EKE and the circulation strength.
- Hydrodynamic instability and interaction with bathymetry as main EKE sources.
- Wind strengthening and the AC curl in fall as an additional forcing.
- Subarctic areas of the heightened energetics due to repeated short-lived structures.
- No prevalence of zonal or meridional EKE.
- QB and interannual variability but no trends covering the whole record.

Limitations of the study: LF portion of geostrophic EKE,
spatial scales > 25 km, temporal scales > 3-4 months.